XXI ENTAC – Encontro Nacional de Tecnologia do Ambiente Construído
14 a 16 de outubro de 2026 | Goiânia-Brasil
DOI: https://doi.org/10.46421/entac.v21i1.8781

Spatiotemporal evolution of the surface urban heat island in Teresina, Piauí, Brazil, using remote sensing data (1995–2025)

Evolução espaço-temporal da Ilha de Calor Urbana de Superfície em Teresina, Piauí, Brasil, a partir de dados de sensoriamento remoto (1995–2025)

Roseana Martins Ribeiro
UFSC | Florianópolis | Brasil | roseanamr@gmail.com
Fernando da Silva Almeida
UFSC | Florianópolis | Brasil | fernando.almeida@labtucal.ufsc.br
Martin Gabriel Ordenes Mizgier
UFSC | Florianópolis | Brasil | martin.ordenes@ufsc.br

Resumo
A intensificação da urbanização tem contribuído para o aumento das temperaturas nas cidades, conforme evidenciado pelo fenômeno da Ilha de Calor Urbana de Superfície (SUHI). Nesse contexto, este estudo analisa a evolução espaço-temporal da SUHI em Teresina, Piauí, Brasil, entre 1995 e 2025. A metodologia incluiu: caracterização da área de estudo; aquisição e processamento de dados Landsat; estimativa da Temperatura da Superfície Terrestre (LST); cálculo dos índices NDVI e NDBI; análise dos mapas; e análise de correlação. Os dados de setembro a dezembro, período mais quente, foram processados no Google Earth Engine. Os resultados indicam aumento na intensidade e extensão da SUHI ao longo das décadas, associado à expansão das áreas construídas e à redução da vegetação. Observou-se relação negativa entre LST e NDVI e positiva entre LST e NDBI, evidenciando o papel da urbanização no clima urbano local. Este estudo reforça o potencial do sensoriamento remoto para análises multitemporais do clima urbano.

Palavras-chave: Ilha de Calor Urbana de Superfície. Sensoriamento remoto. Temperatura da Superfície Terrestre. NDVI. NDBI.

Abstract
The intensification of urbanization has contributed to rising temperatures in cities, as evidenced by the SUHI phenomenon. In this context, this study analyzes the spatiotemporal evolution of SUHI in Teresina, Piauí, Brazil, between 1995 and 2025. The methodology included: characterization of the study area; acquisition and processing of Landsat data; estimation of LST; calculation of NDVI and NDBI indices; map analysis; and correlation analysis. Data from September to December, the hottest period, were processed using Google Earth Engine. The results indicate an increase in both the intensity and spatial extent of SUHI over the decades, associated with the expansion of built-up areas and the reduction of vegetation cover. A negative relationship was observed between LST and NDVI, and a positive relationship between LST and NDBI, highlighting the role of urbanization in shaping the local urban climate. This study reinforces the potential of remote sensing for multitemporal urban climate analysis.

Keywords: Surface Urban Heat Island. Remote sensing. Land Surface Temperature. NDVI. NDBI.

RIBEIRO, R. M.; ALMEIDA, F. S.; MIZGIER, M. G. O. Spatiotemporal evolution of the surface urban heat island in Teresina, Piauí, Brazil, using remote sensing data (1995–2025). In: ENCONTRO NACIONAL DE TECNOLOGIA DO AMBIENTE CONSTRUÍDO, 21, 2026, Goiânia. **Anais**... Goiânia: ANTAC, 2026.

INTRODUCTION

RESEARCH BACKGROUND

Urban growth, intensified by rural-to-urban migration, is expected to increase the share of the world's population living in cities from 55% today to 68% by 2050 [1]. This expansion replaces natural landscapes with impervious artificial surfaces and increases anthropogenic heat emissions from buildings, transportation, and industrial activities, contributing to higher air and surface temperatures, changes in atmospheric humidity, and modifications in local wind circulation [2].

Changes in these parameters result in Urban Heat Islands (UHI), where urban air and surface temperatures are higher than in adjacent rural or peri-urban areas. UHIs increase cooling energy demand, degrade air quality, intensify thermal stress, and aggravate heat-related health problems [3]. These effects are more evident in low-income and rapidly urbanizing regions, where inadequate planning, heterogeneous built surfaces, and limited green infrastructure intensify socio-environmental vulnerability and thermal impacts [4].

In this context, cities in the Global South are among the most susceptible to the effects of UHI due to the combination of the aforementioned factors [5]. Their predominance in tropical and subtropical zones, characterized by high solar radiation and year-round temperatures, further increases their climatic sensitivity [6]. Given this context, mitigating the impacts associated with UHI represents one of the main contemporary challenges for sustainable urban planning and for adapting cities to climate change.

To address these issues, orbital remote sensing has been widely used to assess the thermal vulnerability of urban areas. Landsat thermal observations are among the most established approaches for characterizing high-resolution surface heat patterns and diagnosing Surface Urban Heat Island (SUHI) intensity. However, SUHI analysis requires integrating Land Surface Temperature (LST) with land cover patterns, since surface heat distribution is directly associated with vegetation, soil imperviousness, and built-up expansion [7].

In this context, complementary spectral indices, such as the Normalized Difference Vegetation Index (NDVI) and the Normalized Difference Built-up Index (NDBI), have been widely employed to assess the influence of vegetation cover, evapotranspiration, and built-up density on the urban microclimate, as well as to map the expansion of urbanized surfaces [8].

RESEARCH GAP AND OBJECTIVE

Although studies have highlighted the importance of investigating UHIs and established global climate patterns on this topic, gaps still remain regarding cities in the Global South [9]. Hussainzad and Gou [10] indicate that scientific evidence remains fragmented and spatially uneven compared with cities in the Global North.

In this context, the city of Teresina reflects these structural conditions, making it a relevant case for investigating urban thermal dynamics in rapidly growing tropical

cities. Over recent decades, the municipality's urban area expanded from 110.17 km² to 156.27 km², an increase of 46.10 km². This process has occurred predominantly in a horizontal manner, a pattern often associated with limitations in urban planning and the insufficient incorporation of environmental and urban infrastructure criteria [11]. This dynamic tends to intensify vegetation loss, soil imperviousness, and impacts on the local urban climate.

Therefore, this study aims to analyze the spatiotemporal evolution of the Surface Urban Heat Island in the municipality of Teresina between 1995 and 2025, as an expression of changes in the local urban climate resulting from the urbanization process. To this end, it seeks to assess the influence of changes in land cover and land use on surface thermal patterns, based on multitemporal remote sensing data integrated with the NDVI and NDBI indices.

METHOD

STUDY AREA

The study area comprises the municipality of Teresina, located in the state of Piauí, Northeastern Brazil, at the coordinates 05°05'20" S and 42°48'07" W (Figure 1). The municipality has an approximate territorial area of 1,387.466 km² and an estimated population of 905,692 inhabitants for the year 2025 [12].

Figure 1: Location map of the study area, Teresina-PI, Brazil

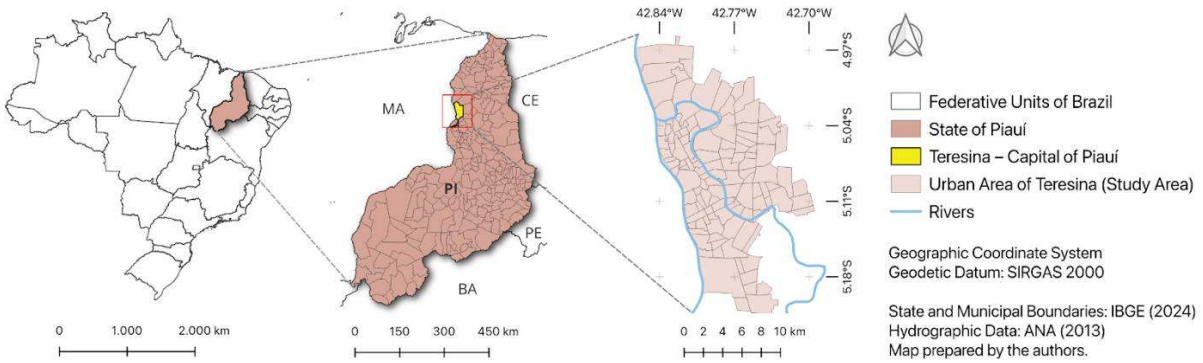

Source: the authors.

According to the climate classification, the municipality has an Aw climate type, characterized as a tropical savanna climate, with two well-defined seasons: a rainy summer and a dry winter [13]. Data from the National Institute of Meteorology indicate that the period between September and December corresponds to the highest thermal intensity in the region, with average maximum temperatures around 38 °C and average relative humidity of approximately 57% [14].

DATA ACQUISITION AND DATA PROCESSING

The data used in this study were obtained from the Landsat series, provided by the United States Geological Survey (USGS), and processed on the Google Earth Engine (GEE) [15]. Landsat Collection 2 (C2), Level 2 (L2) images, previously processed by the

USGS, were used. These products include atmospherically corrected surface reflectance data and surface temperature data [16].

The years 1995, 2005, 2015, and 2025 were analyzed using images from the Landsat 5 TM (Thematic Mapper) sensor for 1995 and 2005, and from the Landsat 8 OLI/TIRS (Operational Land Imager/Thermal Infrared Sensor) sensor for 2015 and 2025. The images correspond to path 219 and rows 63 and 64. The optical bands used to calculate the spectral indices have a spatial resolution of 30 m.

The images with cloud cover below 10% were selected and the pixel quality mask (QA_PIXEL) was applied to remove clouds, shadows, and atmospheric noise. Temporal compositing was then performed using the median pixel value to reduce extreme values and generate a more stable representation of surface conditions.

The analysis period was restricted to September–December, the interval of highest thermal intensity in the region, marked by high solar radiation and low relative humidity. These conditions reduce cloud interference and seasonal variability, favoring the detection of SUHI dynamics. Thus, the median composite was applied to enable comparison among the analyzed years under more homogeneous climatic conditions. In total, 28 images were used, selected based on criteria of temporal consistency and low cloud cover, as shown in Table 1.

Table 1: Details of Landsat datasets from Teresina-PI, Brazil

Year	Product Identifier	Data and Time	Cloud Cover (%)
1995	LT05_L2SP_219063_19950916_20200912_02_T1	1995-09-16 12:01	0.0
	LT05_L2SP_219064_19950916_20200912_02_T1	1995-09-16 12:01	0.0
	LT05_L2SP_219064_19951018_20200912_02_T1	1995-10-18 11:59	0.0
2005	LT05_L2SP_219063_20050911_20200901_02_T1	2005-09-11 12:47	1.0
	LT05_L2SP_219063_20050927_20200901_02_T1	2005-09-27 12:47	0.0
	LT05_L2SP_219063_20051013_20200901_02_T1	2005-10-13 12:47	2.0
	LT05_L2SP_219063_20051029_20200901_02_T1	2005-10-29 12:47	0.0
	LT05_L2SP_219064_20050911_20200901_02_T1	2005-09-11 12:47	0.0
	LT05_L2SP_219064_20050927_20200901_02_T1	2005-09-27 12:47	1.0
	LT05_L2SP_219064_20051029_20200901_02_T1	2005-10-29 12:47	0.0
2015	LC08_L2SP_219063_20150923_20200908_02_T1	2015-09-23 12:59	2.02
	LC08_L2SP_219063_20151009_20200908_02_T1	2015-10-09 12:59	3.15
	LC08_L2SP_219063_20151025_20200908_02_T1	2015-10-25 12:59	0.03
	LC08_L2SP_219063_20151110_20200908_02_T1	2015-11-10 12:59	1.88
	LC08_L2SP_219063_20151126_20200908_02_T1	2015-11-26 12:59	0.47
	LC08_L2SP_219063_20151212_20200908_02_T1	2015-12-12 12:59	6.71
	LC08_L2SP_219064_20150923_20200908_02_T1	2015-09-23 12:59	1.42
	LC08_L2SP_219064_20151025_20200908_02_T1	2015-10-25 12:59	0.21
	LC08_L2SP_219064_20151212_20200908_02_T1	2015-12-12 12:59	8.04
2025	LC08_L2SP_219063_20250902_20250912_02_T1	2025-09-02 12:59	2.16
	LC08_L2SP_219063_20250918_20250929_02_T1	2025-09-18 12:59	0.42
	LC08_L2SP_219063_20251004_20251115_02_T1	2025-10-04 12:59	5.9
	LC08_L2SP_219063_20251020_20251120_02_T1	2025-10-20 12:59	9.5
	LC08_L2SP_219063_20251105_20251126_02_T1	2025-11-05 12:59	3.31
	LC08_L2SP_219064_20250902_20250912_02_T1	2025-09-02 12:59	0.15
	LC08_L2SP_219064_20250918_20250929_02_T1	2025-09-18 12:59	0.0
	LC08_L2SP_219064_20251004_20251115_02_T1	2025-10-04 12:59	0.01
	LC08_L2SP_219064_20251105_20251126_02_T1	2025-11-05 12:59	1.49

Source: the authors.

The number of images varied among the analyzed years, ranging from 3 scenes in 1995 to 9 scenes in 2025, reflecting the limitations of the historical Landsat archive according to the selection criteria. Nevertheless, the 1995 scenes presented 0.0%

cloud cover, ensuring high radiometric quality for this period. The median composite, applied through GEE [15], contributed to minimizing the influence of residual outlier values, thereby reducing the impact of this asymmetry on the results obtained.

LAND SURFACE TEMPERATURE (LST)

LST is an essential parameter for understanding urban thermal conditions and the influence of land cover on SUHI intensification [17]. Besides, SUHI was interpreted as the spatial pattern of higher LST values associated with built-up and impervious surfaces compared with vegetated, water, or less urbanized areas.

In this study, LST was obtained from Landsat C2 L2 products, which provide surface temperature data previously processed by the USGS and corrected for atmospheric effects. Thermal information was extracted from the ST_B6 band for Landsat 5 and the ST_B10 band for Landsat 8, and was subsequently converted from Kelvin to degrees Celsius.

LST products integrate thermal band radiance and physical surface parameters, including emissivity, allowing the estimation of surface thermal patterns. Thus, LST was adopted as the main variable to evaluate urban thermal conditions and support the identification of SUHI in Teresina.

It should be noted that some areas in the LST maps present “No Data” values, associated with limitations of the Landsat C2 L2 product, in which temperature estimation depends on parameters such as surface emissivity and atmospheric conditions. When these parameters cannot be reliably estimated, the pixels are automatically excluded from the product, resulting in data gaps [16].

SPECTRAL INDICES: NDVI AND NDBI

Vegetation cover was analyzed using the NDVI, which is widely used to represent vegetation density and vigor based on the spectral contrast between the red and near-infrared bands [18].

NDVI was calculated according to Equation (1):

$$NDVI = \frac{(NIR - RED)}{(NIR + RED)} \qquad \textit{Equation 1}$$

where *NIR* corresponds to near-infrared reflectance and RED to red reflectance.

Built-up areas were analyzed using the NDBI, which is employed to identify impervious surfaces and urbanized areas based on the spectral response of the shortwave infrared and near-infrared bands [19].

The NDBI was calculated according to Equation (2):

$$NDVI = \frac{(SWIR - NIR)}{(SWIR + NIR)} \qquad \textit{Equation 2}$$

where SWIR represents shortwave infrared reflectance.

Both indices have theoretical values ranging from -1 to +1. For NDVI, higher values indicate greater vegetation density, while values close to zero or negative values are associated with surfaces with low or no vegetation cover, such as exposed soil, built-up areas, and water bodies [18]. For NDBI, positive values tend to indicate a greater presence of built-up or impervious surfaces, while negative values are related to vegetated areas, water bodies, or non-urbanized surfaces [19].

The calculations were performed on the GEE platform using the normalized Difference function, which directly applies the standardized mathematical formulation of these spectral indices.

SPATIOTEMPORAL ANALYSIS

The spatiotemporal analysis was conducted by comparing the LST, NDVI, and NDBI maps for the years 1995, 2005, 2015, and 2025. Comparative analyses between periods were considered, including the identification of spatial trends associated with urban expansion, variations in vegetation cover, and changes in the spatial distribution of land surface temperature. The interpretation integrated visual and spatial analysis of the maps, allowing the identification of critical areas associated with increasing temperature and the intensification of urbanization in Teresina.

The final maps were prepared and standardized in QGIS, where cartographic elements such as legend, graphic scale, and layout were defined, enabling visual standardization and comparability among the different years analyzed**.**

CORRELATION ANALYSIS

To quantify the association between surface thermal patterns and spectral indices, correlation analysis and simple linear regression were applied, following procedures commonly used in SUHI studies to relate LST, spectral indices, and land cover and land use classes [20]. For this purpose, sample points were generated in QGIS across the study area to extract pixel-by-pixel values from the LST, NDVI, and NDBI maps for each year and associate them with land cover classes, including exposed soil, urban areas, vegetation, and water bodies.

The land cover classes were selected based on the main surface types influencing LST variation and following the categories adopted in [20]; class attribution was performed in QGIS through visual interpretation of the thematic maps, supported by NDVI and NDBI patterns.

After extraction in QGIS, the data were exported in CSV format, organized in Microsoft Excel, and used to create LST–NDVI and LST–NDBI scatter plots for the study period. LST was adopted as the dependent variable, while NDVI and NDBI were considered independent variables in separate analyses. The slope coefficient indicated the direction of association, and the coefficient of determination (R^2) was used to assess the proportion of LST variation explained by each spectral index.

DOI: https://doi.org/10.46421/entac.v21i1.8781

RESULTS AND DISCUSSION

SPATIOTEMPORAL EVOLUTION OF URBAN THERMAL PATTERNS AND SUHI

The spatiotemporal evolution of urban thermal trends in Teresina was analyzed through the distribution of LST and its relationship with vegetation cover (NDVI) and built-up areas (NDBI). This integrated approach allows SUHI to be interpreted not only as a spatial thermal variation but also as a pattern resulting from land cover and land use over time. Figure 2 presents the spatial distribution of LST, NDVI, and NDBI for the analyzed years, highlighting the evolution of thermal patterns in the study area.

Figure 2: Spatiotemporal evolution of LST, NDVI, and NDBI in Teresina (PI), for 1995, 2005, 2015, and 2025

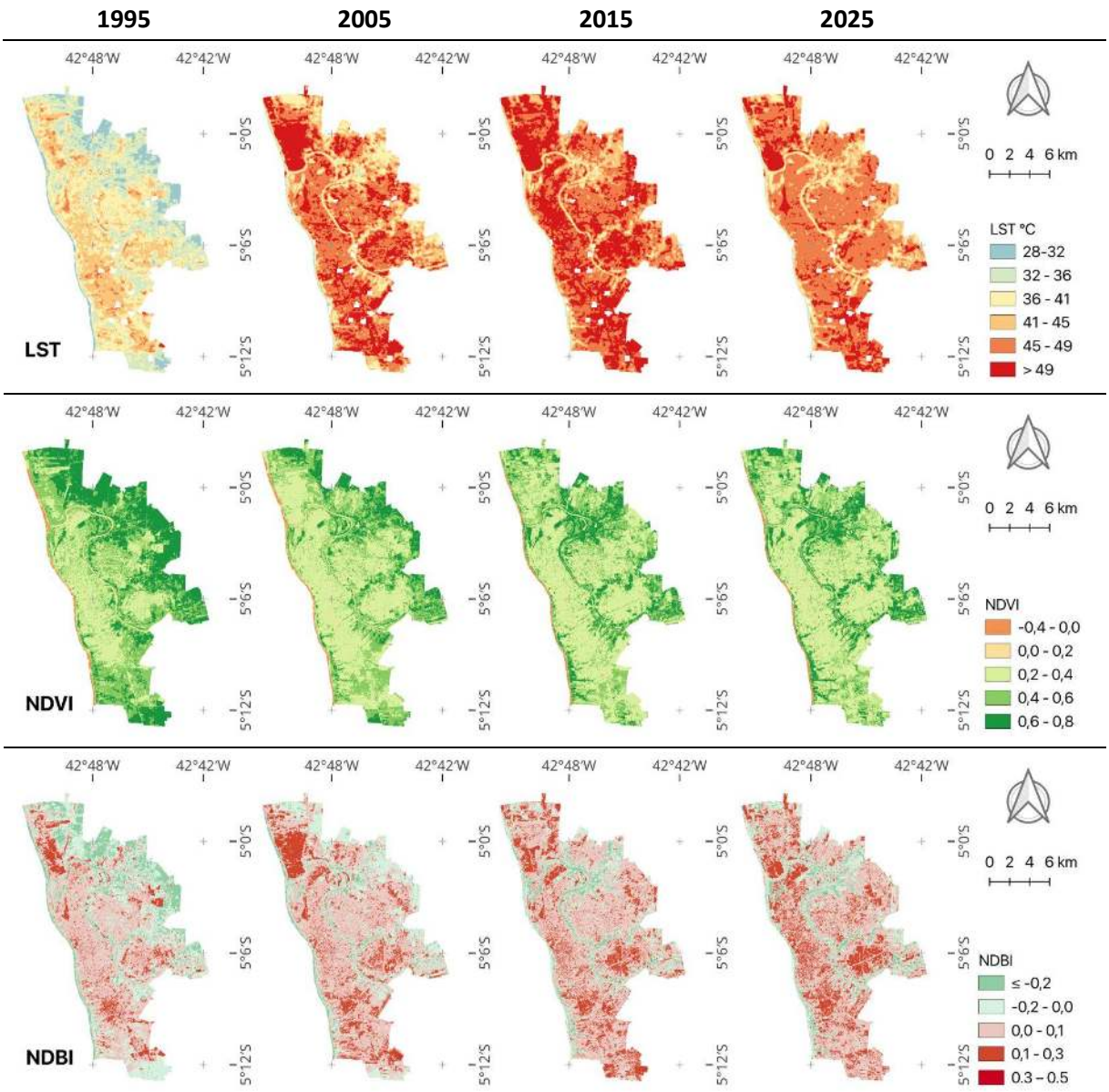

Source: the authors, based on remote-sensing analysis of Landsat images.

The integrated analysis indicates SUHI intensification in Teresina between 1995 and 2025. In 1995, moderate temperatures predominated, between 32 and 41 °C. From 2005 onward, areas with high LST increased, particularly at 45–49 °C and >49 °C. In

2015, these areas occupied more continuous portions of the urban fabric, indicating surface warming. In 2025, LST showed a less extreme distribution than in 2015, with lower values >49 °C and greater predominance between 41 and 49 °C. However, the broad distribution of elevated temperatures in 2025 does not indicate an effective improvement in urban thermal conditions.

This behavior should not be interpreted as a direct reduction in urbanization, but as the result of combined environmental and atmospheric influences on surface thermal response. Remote sensing-derived LST may vary according to soil moisture, antecedent precipitation, atmospheric conditions during satellite overpass, seasonality, and temporal image composition [21].

The distribution of NDVI reinforces the relationship between vegetation and LST. In 1995, the highest values, between 0.4 and 0.8, indicate greater vegetation cover, especially in peripheral areas and near river corridors. Over the study period, a reduction and fragmentation of these areas can be observed, along with the expansion of lower NDVI values, between 0.0 and 0.4, mainly in central areas and urban expansion sectors. In 2015 and 2025, denser vegetation appears in a more restricted pattern, while the consolidated urban area presents lower NDVI values, favoring greater surface exposure and thermal intensification in urbanized sectors.

The NDBI indicates the expansion of built-up or exposed surfaces over the study period. In 1995, positive values appeared in a more fragmented pattern, whereas from 2005 onward they became more pronounced in the northern, central, and southern regions, following areas with higher LST. In 2015 and 2025, these values indicate the consolidation of urban occupation and its expansion into peripheral sectors, in agreement with [11], who identified marked growth of the peripheral urban area of Teresina between 2002 and 2022.

Overall, the results show that SUHI in Teresina results from the interaction between urban expansion, exposed soil, and vegetation loss. The association between higher LST, positive NDBI, and lower NDVI indicates that surface warming is not limited to densely built-up areas, but also occurs on exposed and sparsely vegetated surfaces. In Teresina's context of high temperatures and water seasonality, this reinforces the importance of urban vegetation for thermal mitigation.

CORRELATION ANALYSIS

The correlation analysis (Figure 3) complements the spatial interpretation of the maps by evaluating the relationship between LST, NDVI, and NDBI. For the graphical analysis, the sample points were grouped into simplified land cover classes: Barren, Urban, Vegetation, and Water, based on NDVI and NDBI values, according to the thresholds defined in the methodology.

The results indicate a negative relationship between LST and NDVI in all years, showing that areas with greater vegetation cover tend to present lower land surface temperatures. The negative slope of the regression lines confirms this trend, indicating a reduction in LST as NDVI values increase. This relationship was more expressive in 1995, with $R^2 = 0.2651$, and less intense in 2005, 2015, and 2025, with $R^2 = 0.108, 0.079,$

and 0.122, respectively. The lower R^2 values observed in the later years indicate that vegetation explains a limited proportion of LST variability, particularly as the urban surface becomes more heterogeneous. Similar associations between urban expansion, vegetation loss, and increased LST have also been reported for other tropical Brazilian cities, such as Maceió [22].

For NDBI, a positive relationship with LST was observed in all years, stronger than the relationship observed between LST and NDVI. In this case, the positive slope of the regression lines indicates an increase in LST as NDBI values increase, while R^2 ranged from 0.6416 in 1995 to 0.4873 in 2025, corresponding to approximately 64% and 49% of the variation in LST, respectively. These results reinforce the association between built-up or exposed surfaces and increased land surface temperature.

Figure 3: Relationship between LST with NDVI and NDBI

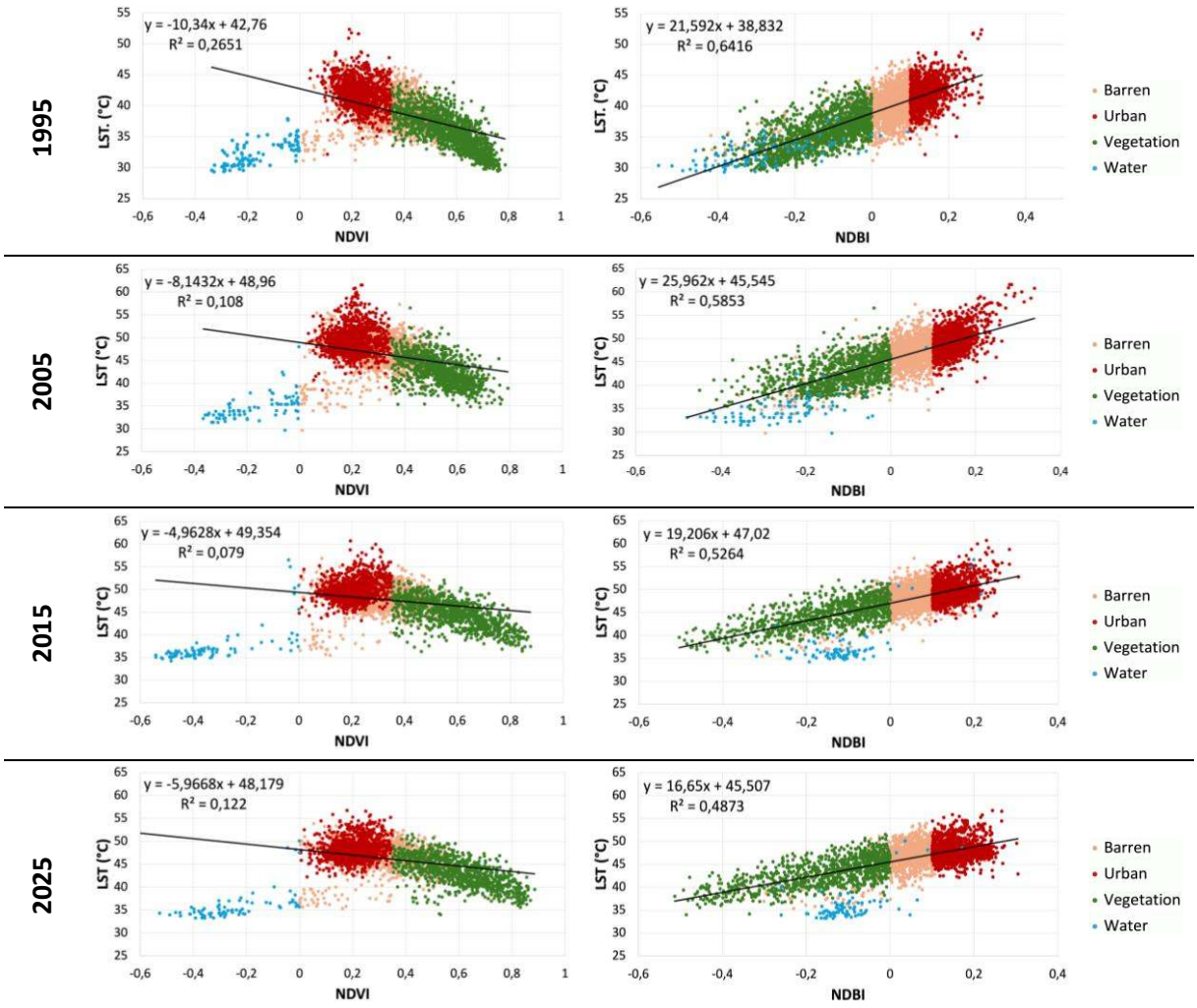

Source: the authors.

Therefore, the distribution of the points confirms the pattern observed in the maps: the Urban and Barren classes concentrate the highest LST values, while Vegetation and Water show lower temperatures. This behavior reinforces the expected relationship in SUHI studies, in which LST tends to decrease with increasing NDVI and to increase with positive NDBI values, as also observed by [20].

CONCLUSION

In view of the problem addressed, the results demonstrate that the SUHI in Teresina intensified over the three decades analyzed, associated with the expansion of built-up and exposed surfaces and the reduction of vegetation cover. The integration of LST, NDVI, and NDBI showed that the highest temperatures are not restricted only to densely urbanized areas, but also occur on sparsely vegetated surfaces and exposed soil, while areas with greater vegetation cover presented more moderate temperatures.

Furthermore, remote sensing proved to be an efficient tool for SUHI mapping, as it enabled the multitemporal analysis of the spatial distribution of LST and its relationship with land cover. The Landsat series, widely used in urban climate studies, reinforces the reliability of this approach due to its temporal continuity and data availability.

Therefore, the results reinforce the need to incorporate climate-sensitive urban strategies into the construction and urban planning guidelines of Teresina, with emphasis on expanding urban vegetation, reducing exposed surfaces, and planning urban expansion areas.

DECLARATION

During the preparation of this article, the authors used artificial intelligence to assist with translating the text into English and improving textual cohesion when necessary. After using the tool, the authors reviewed and edited the content as needed and take full responsibility for the content of the published article.

REFERENCES

[1] D. E. S. A. United Nations, “Population Division World Population Prospects 2019:Highlights.” 2019.

[2] L. Lu, S. Qureshi, Q. Li, F. Chen, and L. Shu, “Monitoring and projecting sustainable transitions in urban land use using remote sensing and scenario-based modelling in a coastal megacity,” *Ocean & Coastal Management*, vol. 224, p. 106201, Jun. 2022, doi: 10.1016/j.ocecoaman.2022.106201.

[3] B. Ju, R. Li, Y. Xu, and B. Huang, “Contrasting Daytime and Nighttime Characteristics and Driving Mechanisms of Surface Urban Heat Islands Across Local Climate Zones—Beijing as a Case Study,” *IEEE J. Sel. Top. Appl. Earth Observations Remote Sensing*, vol. 19, pp. 1567–1582, 2026, doi: 10.1109/JSTARS.2025.3637559.

[4] D. Halder, Harshit, and R. D. Garg, “How spatiotemporal urban expansion shapes heat trends in coastal megacities: Developed vs. developing nations,” *Urban Climate*, vol. 64, p. 102704, Dec. 2025, doi: 10.1016/j.uclim.2025.102704.

[5] S. Jiang *et al.*, “Nonlinear impacts of urban size and vegetation cover on global surface urban heat: Insights from 6022 cities,” *Remote Sensing of Environment*, vol. 333, p. 115154, Jan. 2026, doi: 10.1016/j.rse.2025.115154.

[6] L. Zhao, X. Lee, R. Smith, and K. Oleson, “Strong contributions of local background climate to urban heat islands,” *Nature*, vol. 511, no. 7508, pp. 216–219, Jul. 2014, doi: 10.1038/natureza13462.

[7] Y. Li, B. Han, Y. Peng, and Z. Wang, “Exploration of the spatiotemporal evolution of Surface Urban Heat Island from 2013 to 2023 and driving factors of different years in Tianjin based on Local Climate Zone Scheme,” *Theor Appl Climatol*, vol. 157, no. 1, p. 45, Jan. 2026, doi: 10.1007/s00704-025-05966-2.

[8] D. Bera, N. D. Chatterjee, S. Ghosh, S. Dinda, and S. Bera, “Recent trends of land surface temperature in relation to the influencing factors using Google Earth Engine platform and time series products in megacities of India,” *Journal of Cleaner Production*, vol. 379, p. 134735, Dec. 2022, doi: 10.1016/j.jclepro.2022.134735.

[9] P. K. Diem *et al.*, “Remote sensing for urban heat island research: Progress, current issues, and perspectives,” *Remote Sensing Applications: Society and Environment*, vol. 33, p. 101081, Jan. 2024, doi: 10.1016/j.rsase.2023.101081.

[10] E. A. Hussainzad and Z. Gou, “A machine learning framework for urban heat mitigation in informal settlements: Climate-resilient planning in Kabul, Afghanistan,” *Sustainable Cities and Society*, vol. 133, p. 106845, Oct. 2025, doi: 10.1016/j.scs.2025.106845.

[11] S. Idelano Dantas and V. De Caldas Brito Vieira, “ANÁLISE TEMPORAL DO CRESCIMENTO DA MANCHA URBANA DE TERESINA-PI ENTRE 2002 E 2022,” *Rev. Equa*, vol. 14, no. 1, Dec. 2025, doi: 10.26694/reppggeo.v14i1.8020.

[12] IBGE – INSTITUTO BRASILEIRO DE GEOGRAFIA E ESTATÍSTICA, “Estimativas da população residente para os municípios e para as unidades da federação com data de referência em 1º de julho de 2025.” Rio de Janeiro: IBGE, 2025. Accessed: Apr. 06, 2026. [Online]. Available: https://ftp.ibge.gov.br/Estimativas_de_Populacao/Estimativas_2025/POP2025_20260113.pdf

[13] M. Kottek, J. Grieser, C. Beck, B. Rudolf, and F. Rubel, “World Map of the Köppen-Geiger climate classification updated,” *metz*, vol. 15, no. 3, pp. 259–263, Jul. 2006, doi: 10.1127/0941-2948/2006/0130.

[14] E. A. Bastos and A. S. Andrade Júnior, “Boletim agrometeorológico de 2023 do município de Teresina.” Embrapa Meio-Norte, Teresina, 2024.

[15] N. Gorelick, M. Hancher, M. Dixon, S. Ilyushchenko, D. Thau, and R. Moore, “Google Earth Engine: Planetary-scale geospatial analysis for everyone,” *Remote Sensing of Environment*, vol. 202, pp. 18–27, Dec. 2017, doi: 10.1016/j.rse.2017.06.031.

[16] USGS - UNITED STATES GEOLOGICAL SURVEY, “Landsat 8–9 Collection 2 Level 2 Science Product Guide.” Version 6. Sioux Falls: U.S. Geological Survey, 2023. Accessed: Apr. 06, 2026. [Online]. Available: https://d9-wret.s3.us-west-2.amazonaws.com/assets/palladium/production/s3fs-public/media/files/LSDS-1619_Landsat8-9-Collection2-Level2-Science-Product-Guide-v6.pdf

[17] M. El Kihel, T. Caciora, C. Grava, R.-C. Țarcă, L. Saafadi, and A. Ouallali, “Integrating multi-source remote sensing and ensemble machine learning to quantify the surface urban heat island in Oradea municipality, Romania,” *Urban Climate*, vol. 67, p. 102872, Jun. 2026, doi: 10.1016/j.uclim.2026.102872.

[18] C. J. Tucker, “Red and photographic infrared linear combinations for monitoring vegetation,” *Remote Sensing of Environment*, vol. 8, no. 2, pp. 127–150, May 1979, doi: 10.1016/0034-4257(79)90013-0.

[19] Y. Zha, J. Gao, and S. Ni, “Use of normalized difference built-up index in automatically mapping urban areas from TM imagery,” *International Journal of*

Remote Sensing, vol. 24, no. 3, pp. 583–594, Jan. 2003, doi: 10.1080/01431160304987.

[20] Y. Miky, A. Al Shouny, and A. Abdallah, "Studying the Impact of Urban Management Strategies and Spatiotemporal Dynamics of LULC on Land Surface Temperature and SUHI Formation in Jeddah, Saudi Arabia," *Sustainability*, vol. 15, no. 21, p. 15316, Oct. 2023, doi: 10.3390/su152115316.

[21] K. Jiang *et al.*, "Combined influence of soil moisture and atmospheric humidity on land surface temperature under different climatic background," *iScience*, vol. 26, no. 6, p. 106837, Jun. 2023, doi: 10.1016/j.isci.2023.106837.

[22] W. L. F. Correia Filho, D. D. B. Santiago, J. F. D. Oliveira-Júnior, and C. A. D. Silva Junior, "Impact of urban decadal advance on land use and land cover and surface temperature in the city of Maceió, Brazil," *Land Use Policy*, vol. 87, p. 104026, Sep. 2019, doi: 10.1016/j.landusepol.2019.104026.